Journal of
Materials Chemistry C

Accepted Manuscript

This article can be cited before page numbers have been issued, to do this please use: C. Quinton, S. Chi, C. Dumas-Verdes, P. Audebert, G. Clavier, J. Perry and V. Alain, *J. Mater. Chem. C*, 2015, DOI: 10.1039/C5TC00531K.

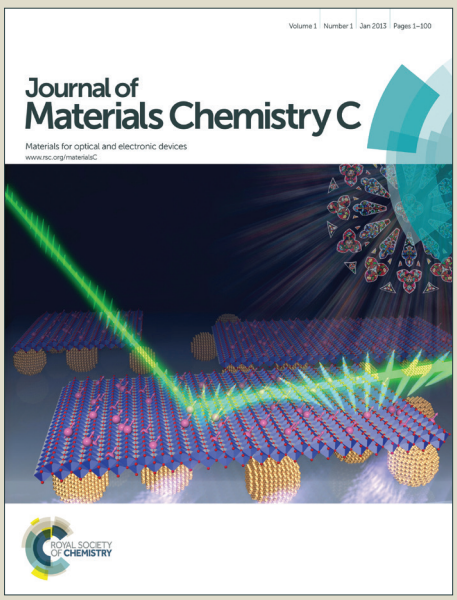

ROYAL SOCIETY OF CHEMISTRY

www.rsc.org/materialsC

View Article Online
DOI: 10.1039/C5TC00531K

Journal Name

ARTICLE

Novel *s*-tetrazine-based dyes with enhanced two-photon absorption cross-section

Received 00th January 20xx,
Accepted 00th January 20xx

DOI: 10.1039/x0xx00000x

www.rsc.org/

Cassandre Quinton,[a] San-Hui Chi,[b] Cécile Dumas-Verdes,[a] Pierre Audebert,[a] Gilles Clavier,[a] Joseph W. Perry,[b*] and Valérie Alain-Rizzo[a*]

This paper reports the synthesis, the linear and non-linear absorption properties of a series of new tetrazine-based D-π-A-π-D and D-π-A type dyes. In these derivatives, a central tetrazine core was connected with one or two terminal triphenylamine moiety(ies) via various π-conjugated spacers. These compounds were efficiently synthesized by Stille or Suzuki-Miyaura cross coupling as a key step. Their photophysical properties, including one-photon absorption and two-photon absorption (2PA), were investigated with special attention to structure-properties relationships. Large 2PA cross-sections (>800 GM) of these tetrazine dyes were evaluated by open aperture z-scan and non-degenerate 2PA techniques. The strong 2PA of these molecules are attributed to the extended π system and to the enhanced intramolecular charge transfer between triphenylamine donor and center tetrazine acceptor.

Introduction

Tetrazine (Tz) is well known as a highly electron-withdrawing group, which can be useful in both optical and electronic applications. The low LUMO energy of tetrazine derivatives enables inverse demand Diels-Alder cycloaddition reactions as a heterodiene[1-13] and stabilizes the anionic intermediate that enables aromatic nucleophilic substitution.[14-19] Tetrazine derivatives are also used in coordination chemistry[20-24] because they can form complexes with electron-rich metals. In addition, some tetrazine derivatives show strong electrofluorochromism[25-32] and have been utilized in pollutant detection.[33]

Recently, it has also been shown that they can be used efficiently as electron carrier in n-type field effect transistors.[34] A theoretical study[35] further predicts a higher polarizability for the diphenyl-*s*-tetrazine compared to triazines, diazines, and pyridine. These findings suggest that tetrazine derivatives could possess large nonlinear optical response and be potential building blocks of nonlinear optical materials for photonic applications. To the best of our knowledge, two-photon absorption cross-sections for tetrazine-based derivatives have not yet been reported.[36, 37]

Studies on the structure-property relationships of nonlinear optical materials have shown that the combination of donor (D) and acceptor (A) groups in molecular frameworks, such as D-π-A,[38-41] D-π-D,[42-44] D-π-A-π-D,[45, 46] can lead to increases in the two-photon absorption (2PA) cross-section (δ, in GM = 1×10^{-50} cm^4 s photon^{-1}), because of D-A coupling that enhances the asymmetrical or symmetrical intramolecular charge transfer (ICT) upon excitation.[45, 46]

In this study, we report the synthesis of charge-transfer *s*-tetrazine-based chromophoric compounds with "push-pull" D-π-A and "push-pull-push" D-π-A-π-D molecular structures and their linear and nonlinear optical properties. Different π conjugated linkers (thiophenylene and phenylene) and substitution patterns on phenylene linkers (Fig. 1) have been used to analyze their contribution to the charge-transfer and electronic delocalization in order to understand their influence on the linear and nonlinear optical properties of the tetrazine based chromophores. The nonlinear optical properties were characterized with femtosecond-pulse z-scan and non-degenerate 2PA (ND-2PA) techniques, since tetrazines of the type studied are not fluorescent. DFT calculations have been carried on all compounds to provide insights for the experimental results.

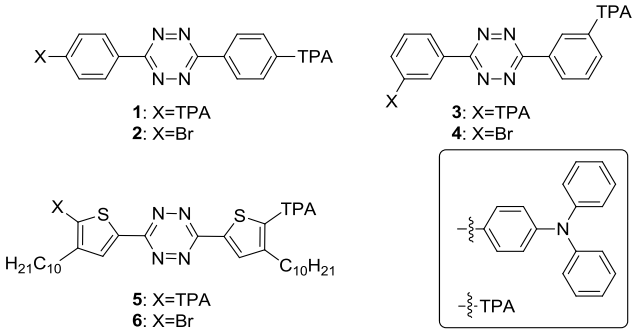

Fig. 1 Tetrazine-based bichromophoric compounds.

[a] PPSM, CNRS UMR8531, ENS Cachan, 61 Avenue du Président Wilson, 94235 Cachan, France
[b] School of Chemistry and Center for Organic Photonics and Electronics, Georgia Institute of Technology, Atlanta, Georgia 30332-0400, USA

Electronic Supplementary Information (ESI) available: absorption spectra, results of TD-DFT calculations, representation of the main molecular orbitals involved in the electronic transitions, atomic coordinates of compounds after geometry optimization. See DOI: 10.1039/x0xx00000x

View Article Online
DOI: 10.1039/C5TC00553K

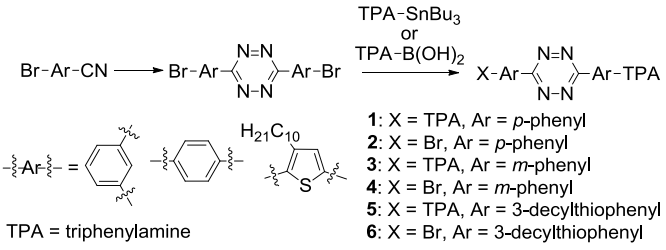

Scheme 1 Synthetic route to tetrazine-based bichromophoric compounds **1**-**6**.

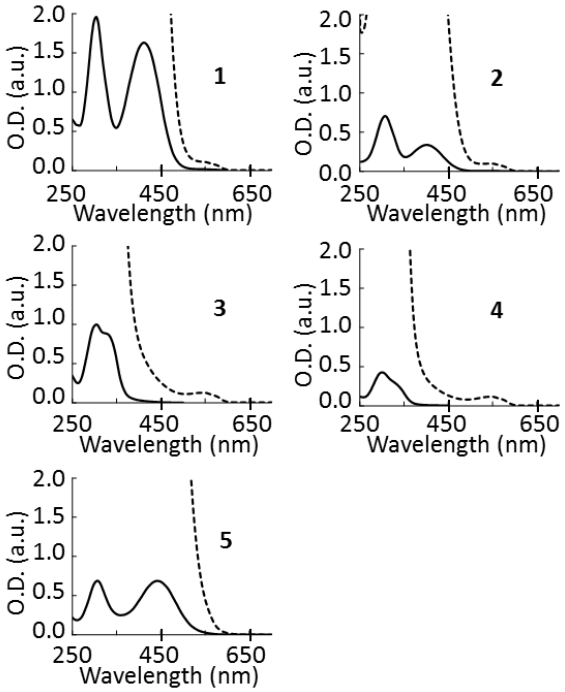

Fig. 3 Linear absorption spectra of tetrazines **1**-**5** (solid line). The dashed line shows the weak n-π* transition ~550 nm.

Table 1. Linear and two-photon absorption properties of tetrazines measured in DCM: absorption wavelength (λ, nm), molar absorption coefficient (ε, L mol^{-1} cm^{-1}), cross-section (δ, GM)

	$\pi_{Tz+link}\rightarrow\pi^*_{Tz+link}$		$\pi_{TPA}\rightarrow\pi^*_{Tz+link}$		$n_{Tz}\rightarrow\pi^*_{Tz}$		2PA	
	λ_1	ε_1	λ_2	ε_2	λ_3	ε_3	$\lambda^{(2)}$	δ
1	303	68000	412	59000	sh		795	860
2	307	47000	401	23000	545	460	840	240
3	304	64000	327	56000	546	540		
4	300	59000	sh		547	570		
5	306	49000	442	49000	-	-	820	650
6	305	35000	441	25000	-	-		
	354	34000						

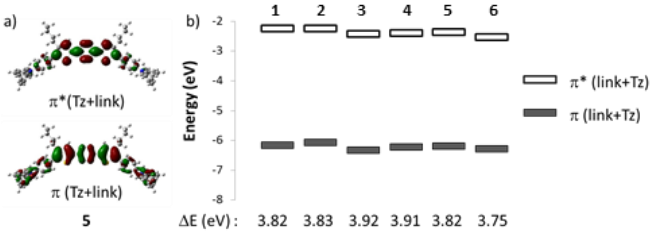

Fig. 4 a) Representation of the main molecular orbitals involved in the π-π* λ_1 electronic transition of **5**; b) Energy levels of the orbitals π(Tz+link) and π*(Tz+link) involved in the π-π* λ_1 electronic transition for compounds **1**-**6**.

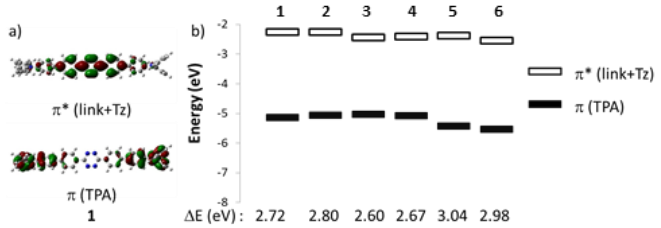

Fig. 2 a) Representation of the main molecular orbitals involved in the ICT π-π* λ_2 electronic transition of **1**; b) Energy levels of the orbitals π(TPA) and π*(link+Tz) involved in the ICT π-π* λ_2 electronic transition for compounds **1**-**6**.

Result and Discussion

Synthesis

Chromophores were synthesized first by the Pinner reaction followed by Stille or Suzuki-Miyaura cross-coupling reactions (Scheme 1, details on the synthetic parts are given in the Supporting Information).

Linear spectroscopic properties

The tetrazine derivatives are yellow or pink and display two or three linear absorption bands in dichloromethane (DCM) solution, as shown in Fig. 2. The linear optical data are reported in Table 1. In order to properly assign the observed electronic transitions, theoretical calculations have been performed at the DFT/B3LYP(3-21g) level for the geometry optimization, and TDDFT/PBE0 (6-31+g(d)) level for the electronic excitation (detailed results given in SI).

The band located at around 305 nm is mainly due to a π-π* transition (λ_1) between molecular orbitals delocalized on the tetrazine core and the linkers (phenylene for **1**, **2**, **3**, **4** and thiophenylene for **5** and **6**) as can be seen in Fig. 3a. This matches with a high extinction coefficient varying from 34000 to 68000 L mol^{-1} cm^{-1} depending on the specific compound. TD-DFT calculation shows that the variation of the energetic gap between these latter orbitals is very small (between 3.75 and 3.92 eV, Fig. 3b) which is in agreement with the experimental results (300 nm < λ_1 < 307 nm, Fig. 2).

Four of the six compounds (**1**, **2**, **5** and **6)** display a distinct intramolecular charge transfer (ICT) band (λ_2) located at around 405 nm in the case of the phenylene linker (**1** and **2**) and at 441 nm in the case of the thiophenylene linker (**5** and **6**). Its molar absorptivity is doubled for **1** and **5** (which contain two triphenylamine moieties) compared to the monosubstituted compounds **2** and **6**. Theoretical calculations show that this band is due to a transition from a π-orbital localized on the triphenylamine unit to a π*-orbital localized on the tetrazine core and the linker (Fig. 4a). As the thiophenylene linker has lower aromaticity and thus a smaller charge-transfer barrier,

View Article Online
DOI: 10.1039/C5TC00531K

Table 2. Absorption wavelength (λ_2, nm) of the intramolecular charge transfer band ($\pi_{TPA} \rightarrow \pi_{link+Tz}$) of compound 1, 2, and 5 in different solvents

	cy	DCM	THF	AcOEt	ACN
1	405	412	407	403	400
2	394	401	396	389	385
5	427	442	437	432	430

stronger donor-acceptor electronic coupling between TPA and Tz core of compound **5** and **6** and, therefore, results a further red-shifted ICT band, compared to **1** and **2**. The representations of the calculated electron density changes accompanying this electronic excitation are displayed in the Supporting Information (Fig.S12, Fig.S15, and Fig.S18). Such ICT bands have been observed for tetrazine-based derivatives functionalized with donors.[19, 47] In the case of the compounds **3** and **4**, the donor unit and tetrazine moiety are in a *meta*-position on the phenylene linker resulting in reduced conjugation lengths, compared to *para*-substituted compounds **1** and **2**. The ICT band is likely blue shifted to around 330 nm because of the change in conjugation and the spectral overlap with the π(Tz+link)$\rightarrow\pi^*$(Tz+link) band.

The ICT band shows weak solvatochromism (Table 2): as solvent polarity increased, from apolar cyclohexane (cy) to moderate polar DCM, bathochromic shift of this ICT absorption is observed. As the solvent polarity continuously increased, from DCM, tetrahydrofurane (THF), ethyle acetate (AcOEt), to acetonitrile (ACN), this ICT absorption is hypsochromically shifted. A similar change has been reported on the donor-acceptor compound 3-chloro-6-tetrathiafulvalene-*s*-tetrazine.[47] The solvent-dependent ICT absorption was further analyzed with Eq. (1) based on four empirical scales including the solvent polarizability (SP), dipolarity (SdP), acidity (SA) and basicity (SB):[48]

$$\bar{\nu} = \bar{\nu}^{\circ} + aSP + bSdP + cSA + dSB \quad (1)$$

where $\bar{\nu}$ is the absorption wavenumber and $\bar{\nu}^{\circ}$ is the gas phase wavenumber. The regression coefficients *a*, *b*, *c* and *d* describe the roles of these four empirical scales in observed solvent effect. In the case of compound **1**, for example, it appears that this chromophore presents a solvatochromism dominated by solvent polarizability (a = -3715, b = 118, c = 91, d = 157, r^2 = 0.87), as observed in other charge transfer molecules.[49, 50]

The band located around 550 nm is assigned to the very weak n-π^* transition[51] (λ_3) localized on the tetrazine core (Fig. 5a) based on the results of the calculation. The location of this band varies slightly amongst the compounds. This result is in agreement with the observations for other tetrazine-based derivatives.[14, 15,52]

Nonlinear spectroscopic properties

Based on linear spectroscopy and theoretical calculations, the compounds **1**, **2**, **5** and **6** seem to be good candidates for two-photon absorption and particularly **1** and **5** which are

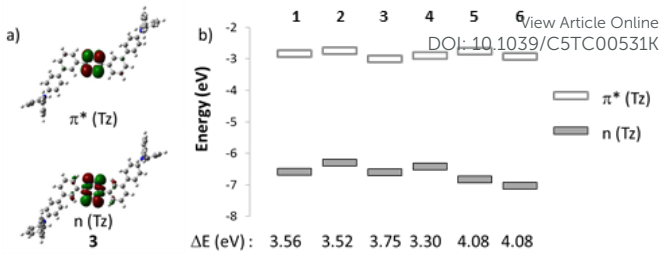

Fig. 5 a) Representation of the main molecular orbitals involved in the n-π^* λ_3 electronic transition of **3**; b) Energy levels of the orbitals n(Tz) and π^*(Tz) involved in the n-π^* λ_3 electronic transition for compounds **1**-**6**.

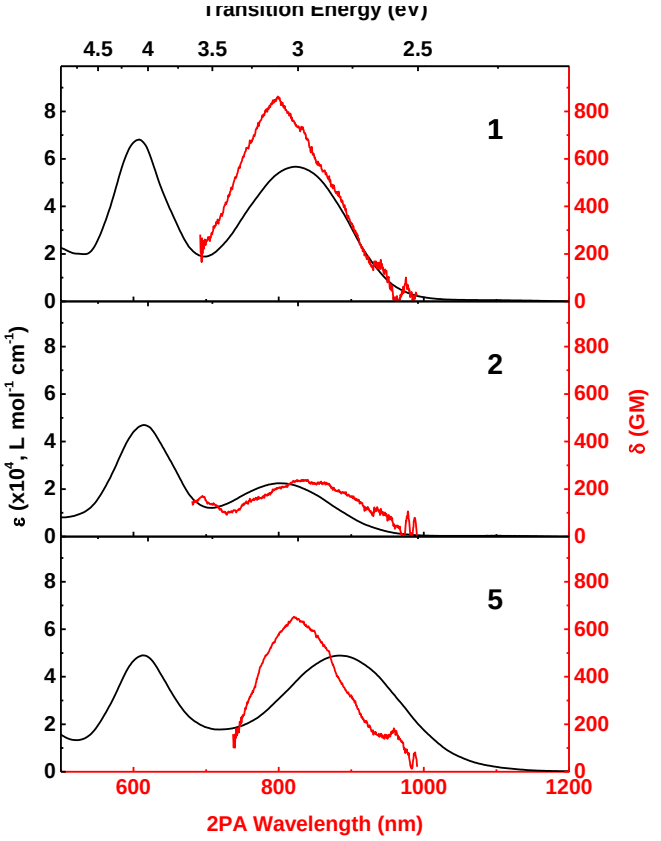

Fig. 6 Linear (black curves, scale upwards) and two-photon (red curves, scale downwards) absorption spectra of **1**, **2** and **5** in DCM.

centrosymmetric or quasi-centrosymmetric and display a very intense ICT band. As shown in Fig. 6, compounds **1**, **2** and **5** showed substantial 2PA in the wavelength range of 700-1000 nm. The corresponding 2PA properties are listed in Table 1. The 2PA spectra of these three samples were mapped by using the ND-2PA technique and the 2PA absorption cross-sections were calibrated and scaled to the values from the open-aperture z-scan measurements.[‡, §, 53, 54] *Meta*-substituted **3** and **4** did not show measurable nonlinear optical response. The difficulties in obtaining highly pure **6** prevented the study of its nonlinear spectroscopic properties.

Both **1** and **5** show sizable peak 2PA cross sections of 860 and 650 GM. For compound **5**, the 2PA cross section is reduced as compared to **1**; this is attributed to the lower symmetry, quasi-linear structure and reduced conjugation length due to

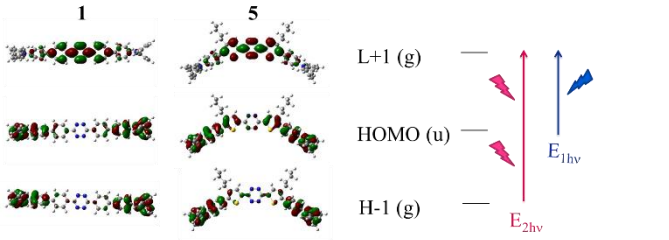

		E_{2hv} (eV)	E_{1hv} (eV)	ΔE_{12} (eV)
1	Exp	3.12	3.01	0.11
	Calc	2.81	2.68	0.13
5	Exp	3.02	2.81	0.21
	calc	2.76	2.56	0.20

E_{1hv} (exp) = hv_{ICT}
E_{2hv} (exp) = $2\times hv_{mes}$
E_{1hv} (calc) = $E_{L+1} - E_{HOMO}$
E_{2hv} (calc) = $E_{L+1} - E_{H-1}$
$\Delta E_{12}=E_{2hv} - E_{1hv}$

Fig. 7 Experimental and calculated energy differences between one-photon and two-photon transitions for **1** and **5**. The calculated values come from Table S8 and Table S10.

the large dihedral angle between the decyl-substituted the torsion angle between thiophenylene and phenylene (50°, see Fig. S8 in SI). On the other hand, the large 2PA cross section of **1** benefits from the centrosymmetric, linear conjugated structure and a slightly longer conjugation length, due to the reduced dihedral angle between the phenylene linker and TPA (40°). The contribution of resonance enhancement of the n-π* transition in these tetrazines should be very small, due to the perpendicular geometry of the non-bonding and π* orbitals. However, such a small contribution may still have a role in the pre-resonance enhancement that leads to the larger two-photon cross-section of **1**.

It should be noted that, as shown in Fig. 6 and Fig. 7, the energy gap (ΔE_{12}) between 2PA ($\lambda^{(2)}$) and the ICT ($\pi_{TPA}\rightarrow \pi_{link+Tz}$) linear absorption band (λ_2) are ~0.11 and 0.21 eV for **1** and **5**, respectively. The magnitude of ΔE_{12} of **5** is in the range for most D-A-D molecules[45] studied; on the other hand, that of **1** is peculiarly small. The cause of such small ΔE_{12} for **1** is not completely clear at this point and is tentatively attributed to the large charge-transfer barrier due to the highly aromatic biphenylenes that would reduce the electronic coupling of the amine donors to the tetrazine core. As indicated by TDDFT results, as shown in Fig. 7, the transition at λ_2 and $\lambda^{(2)}$ for **1** and **5** is attributed HOMO → LUMO+1 (u → g) and HOMO-1 → LUMO+1 (g → g) transitions, respectively, and both have strong CT character. The calculated ΔE_{12} between are 0.13 and 0.20 eV for **1** and **5,** respectively, which agree with the experimental energy differences. While both LUMO+1 orbitals of **1** and **5** have near the same energy, the origin of the difference comes from the higher HOMO-1 orbital energy of **1** compared to **5**, which again supports the increased aromaticity and charge transfer barrier giving reduced electronic coupling in **1**. The representations of the calculated electron density changes accompanying both electronic excitations are displayed in the Supporting Information (Fig. S12-S13 for **1**, and Fig. S12-S19 for **5**).

The compound **2**, which is a non-centrosymmetric molecule, displays a two-photon transition 0.14 eV lower than the one-photon ICT transition. Calculations show that there is an extremely weak HOMO → LUMO electronic transition at a lower energy than λ_2 (Δ=0.56eV). The large energy difference can be attributed to the known deficiencies of DFT calculations that underestimate energies of charge transfer states. The contribution of this low-energy CT band could explain the visible red-shifted 2PA. The representations of the calculated electron density changes accompanying these electronic transitions are displayed in the Supporting Information (Fig. S14-S15).

Conclusions

In summary, six linear tetrazine-based chromophores with terminal triphenylamine groups have been designed and synthesized through an efficient procedure. The 2PA cross sections of centrosymmetric and quasi-centrosymmetric compounds **1** and **5**, respectively, are larger than those of quadrupolar and octupolar derivatives based on triphenlyamine and triazole,[55] azoaromatic- or imine-based charge transfer molecules,[56, 57] and common photoinitiators,[58] and are comparable with the vibronically-allowed 2PA of some cyanine dyes.[59, 60] The sizable 2PA is attributed to the significant intramolecular charge-transfer between the strong electron-accepting tetrazine core and the electron-donating triphenylamine groups. Furthermore, the length, planarity, and aromaticity of the π-conjugated spacers (thiophenylene and phenylene) between the tetrazine unit and the triphenylamine group play an important role in increasing the magnitude of the 2PA. This is the first study which clearly highlights functionalized tetrazines for 2PA-related applications, such as optical limiting and 3D microfabrication. Application of these tetrazines in photonic applications is planned for future work and preliminary one-photon polymerization results indicated compound **1** could be a potential two-photon initiator that comparable with stilbene-based initiators[61] that have similar 2PA cross-sections. This study could stimulate the synthesis of new two-photon absorbing materials.

Experimental

Linear and Nonlinear spectroscopic measurements

UV-visible absorption spectra were recorded on a Cary 5000 spectrophotometer in 1 cm optical length quartz cuvettes. Dichloromethane (SDS, spectrometric grade) was employed as the solvent for absorption measurements. For nonlinear spectroscopic measurements, samples were prepared in dichloromethane (Sigma-Aldrich, spectral grade) with the averaged concentration of ~1 mM. For ND-2PA measurements, excitation wavelength of 1300 nm and a white light continuum (WLC) probe ranging from 400-750 nm were selected to acquire the ND-2PA spectra from 600-1000 nm. The two-photon wavelengths are obtained with Eq. (2).

$$\lambda_{ND2PA} = \frac{2}{\lambda_{pump}^{-1} + \lambda_{probe}^{-1}} \quad (2)$$

View Article Online
DOI: 10.1039/C5TC00551K

where λ_{pump} and λ_{probe} are the excitation and probing wavelengths respectively. The optical pathlength of sample cuvette for ND-2PA measurements is 2 mm. For z-scan measurements, a near Gaussian beam at 830 nm with $M^2 \sim 1.09$, beam waist $\omega(HW_{1/e2}) \sim 40$ μm, and pulse width $\tau_p(HW_{1/e}) \sim 60$ fs was used. The excitation irradiance ranges from 33–280 GW/cm^2. The optical pathlength of sample cuvettes for z-scan measurements is 1 mm.

Quantum chemical calculations

Calculations were performed with the Gaussian 03 at the MESO calculation centre of the ENS Cachan (Nec TX7 with 32 processors of type Itanium 2). Molecules were drawn with the Gaussview 03 software using included templates and their geometry optimized at the B3LYP/3-21+g(d) level of theory. Infrared spectra were calculated on the final geometry to ascertain that a minimum was obtained (no negative frequencies). Time-dependant density functional theory (TD-DFT) calculations at the PBE0 level of theory with the 6-31+g(d) basis set were subsequently performed.

Synthesis

Reagents were commercially available from Aldrich and used without further purification. Syntheses of the intermediary compounds are described in the Supporting Information. Column chromatography was performed with SDS 0.040-0.063 mm silica gel. All compounds were characterized by the usual analytical methods: ^{1}H, ^{13}C NMR spectra were recorded with a JEOL ECS (400 MHz) spectrometer. All chemical shifts are referenced to the solvent peak (J values are given in Hz). Melting points were measured with a Kofler melting-point apparatus. IR spectra were recorded with a Nicolet Avatar 330 FT-IR spectrometer. This work has benefited from the facilities and expertise of the Small Molecule Mass Spectrometry platform of IMAGIF (Centre de Recherche de Gif - www.imagif.cnrs.fr).

General procedure for Stille cross-coupling. Dibromophenyltetrazine compound (1.0 eq, 0.1 M) and *N,N*-diphenyl-4-tributyltinaniline (1.1 eq for monosubstitution and 3.0 eq for disubstitution) were dissolved in toluene (for **3** and **4**) or THF (for **1** and **2**). [Pd(PPh$_3$)$_4$] (5 mol% for each substitution) was added and the reaction mixture was refluxed for 10 hours (for **3** and **4**) or 100 hours (for **1** and **2**) under argon. 30 mL of a solution of potassium fluoride (10% in water) was added and the precipitate was removed by filtration on celite. The filtrate was extracted with diethylether (2×50mL), the organic layer was washed with water (100 mL) and dried over anhydrous sodium sulfate Na_2SO_4, filtrated and concentrated under reduced pressure. The crude product was purified by a silicagel column chromatography to give an orange solid.

3,6-bis(*N*,*N*-diphenyl-4'-biphenylamine)-*s*-tetrazine (1). General procedure for Stille cross-coupling with 3,6-bis(4'-bromophenyl)-*s*-tetrazine (0.21 g, 0.53 mmol). Chromatography conditions: CH_2Cl_2/PE (9/1)-CH_2Cl_2; Yield: 24% (71 mg); mp: 102 °C; IR (ν_{max}/cm^{-1}): 1483, 1271; ^{1}H NMR (400 MHz, $CDCl_3$) δ (ppm): 8.70 (d, J=8.2 Hz, 4H), 7.82 (d, J=8.2 Hz, 4H), 7,59 (d, J=8.7 Hz, 4H), 7,30 (dd, J=8.2 and 7.3 Hz, 8H), 7.19-7.15 (m, 12H), 7.07 (t, J=6.9 Hz, 4H); ^{13}C NMR (100 MHz, $CDCl_3$) δ (ppm): 163.8; 148.3; 147.6; 144.9; 133.3; 131.7; 129.5; 128.5; 128.0; 127.4; 124.9; 123.5 (2C); HRMS-ESI (m/z): (M+H)$^+$ calcd for $C_{50}H_{36}N_6$, 721.3080, found: 721.3079; UV-vis (CH_2Cl_2) $\lambda_{max}(\varepsilon)$ = 304 nm (70700 L.mol^{-1}.cm^{-1}) and 412 nm (58600 L.mol^{-1}.cm^{-1})

3-(4'-bromophenyl),6-(*N*,*N*-diphenyl-4'-biphenylamine)-*s*-tetrazine (2). General procedure for Stille cross-coupling with 3,6-bis(4'-bromophenyl)-*s*-tetrazine (0.60 g, 1.5 mmol). Chromatography conditions: CH_2Cl_2/PE (5/5)-CH_2Cl_2; Yield: 19% (159 mg); mp: 258 °C; IR (ν_{max}/cm^{-1}): 3031-2917, 1604, 1584, 1496, 1433, 1355, 1317, 1274, 1174, 1155, 1060, 916, 819; ^{1}H NMR (400 MHz, $CDCl_3$) δ (ppm): 8.69 (d, J=8.7 Hz, 2H), 8.53 (d, J=8.2 Hz, 2H), 7.82 (d, J=8.2 Hz, 2H), 7.76 (d, J=8.2 Hz, 2H), 7.59 (d, J=8.2 Hz, 2H), 7.30 (d, J=7.8 and 7.3 Hz, 4H), 7.17 (d, J=8.7 Hz, 2H), 7.16 (d, J=8.7 Hz, 4H), 7.07 (dt, J=7.3 and 0.9 Hz, 2H); ^{13}C NMR (100 MHz, $CDCl_3$) δ (ppm): 164.1; 163.4; 148.4; 147.5; 145.1; 133.2; 132.9; 132.8; 131.0; 129.5; 129.4; 128.7; 128.0; 127.9; 127.4; 125.0; 123.5; 123.4; HRMS-ESI (m/z): (M+H)$^+$ calcd for $C_{32}H_{22}N_5{}^{79}Br$, 556.1131, found: 556.1140; UV-vis (CH_2Cl_2) $\lambda_{max}(\varepsilon)$ = 307 nm (61000 L.mol^{-1}.cm^{-1}) and 401 nm (30100 L.mol^{-1}.cm^{-1})

3,6-bis(*N*,*N*-diphenyl-3'-biphenylamine)-*s*-tetrazine (3). General procedure for Stille cross-coupling with 3,6-bis(3'-bromophenyl)-*s*-tetrazine (0.61 g, 1.6 mmol) Chromatography conditions: cyclohexane/toluene: 5/5; Yield: 19% (217 mg); mp: 92 °C; IR (ν_{max}/cm^{-1}): 2920, 1587, 1515, 1483, 1382, 1271, 918, 835; ^{1}H NMR (400 MHz, $CDCl_3$) δ (ppm): 8.91 (dd, J=1.8 and 1.8 Hz, 2H), 8.60 (ddd, J=7.8, 1.8 and 1.8 Hz, 2H), 7.85 (ddd, J=7.8, 1.8 and 0.9 Hz, 2H), 7.66 (dd, J=7.8 and 7.8 Hz, 2H), 7.61 (d, J=8.7 Hz, 4H), 7.31 (dd, J=8.7 and 7.3 Hz, 8H), 7.21-7.17 (m, 12H), 7.08 (dt, J=7.3 and 1.4 Hz, 4H); ^{13}C NMR (100 MHz, $CDCl_3$) δ (ppm): 164.1, 147.9, 147.7, 141.8, 133.8, 132.3, 130.8, 129.9, 129.5, 128.0, 126.3, 126.1, 124.7, 123.8, 123.3; HRMS-ESI (m/z): (M+H)$^+$ calcd for $C_{50}H_{36}N_6$, 721.3080, found: 721.3098; UV-vis (CH_2Cl_2) $\lambda_{max}(\varepsilon)$ = 304 nm (64000 L.mol^{-1}.cm^{-1}) and 546 nm (540 L.mol^{-1}.cm^{-1})

3-(3'-bromophenyl),6-(*N*,-diphenyl-3'-biphenylamine)-*s*-tetrazine (4). General procedure for Stille cross-coupling with 3,6-bis(3'-bromophenyl)-*s*-tetrazine (0.20 g, 0.51 mmol). Chromatography conditions: cyclohexane/toluene: 5/5; Yield: 28% (80 mg); mp: 205 °C; IR (ν_{max}/cm^{-1}): 3034-2917, 1586, 1495, 1485, 1438, 1383, 1356, 1317, 1273, 915, 820; ^{1}H NMR (400 MHz, $CDCl_3$) δ (ppm): 8.87 (s, 1H), 8.81 (s, 1H), 8.59-8.56 (m, 2H), 7.84 (d, J=7.8 Hz, 1H), 7.76 (d, J=7.8 Hz, 1H), 7.65 (dd, J=7.8 and 7.8 Hz, 1H), 7,59 (d, J=8.7 Hz, 2H), 7,48 (dd, J=7.8 and 7.8 Hz, 1H), 7,31 (dd, J=8.2 and 7.3 Hz, 4H), 7.20-7.16 (m, 6H), 7.07 (t, J=7.3 Hz, 2H); ^{13}C NMR (100 MHz, $CDCl_3$) δ (ppm): 164.3, 163.1, 147.9, 147.6, 141.9, 135.6, 133.9, 133.7, 132.1, 131.1, 130.9 (2C), 129.9, 129.5, 127.9, 126.5, 126.4, 126.2, 124.7, 123.7, 123.6, 123.3; HRMS-ESI (m/z): (M+H)$^+$ calcd for $C_{32}H_{22}N_5{}^{79}Br$, 556.1131, found: 556.1134; UV-vis (CH_2Cl_2) $\lambda_{max}(\varepsilon)$ = 300 nm (59000 L.mol^{-1}.cm^{-1}) and 547 nm (570 L.mol^{-1}.cm^{-1})

4,4'-(5,5'-(*s*-tetrazine-3,6-diyl)bis(3-decylthiophene-5,2-diyl))bis(*N*,*N*-diphenylaniline) (5) and 4-(5-(6-(5-bromo-4-decylthiophen-2-yl)-*s*-tetrazin-3-yl)-3-decylthiophen-2-yl)-*N*,*N*-diphenylaniline (6). To a solution of 3,6-bis(5-bromo-4-decylthiophen-2-yl)-*s*-tetrazine (0.25 g, 0.37 mmol, 1.0 eq) and tetrakis(triphenylphosphine) palladium(0) Pd(PPh$_3$)$_4$ (21 mg,

0.019 mmol, 5 mol%) in toluene (5 mL) were added first a solution of triphenylamine boronic acid (0.24 g, 0.84 mmol, 2.3 eq) in methanol (1.5 mL) and then a aqueous solution of sodium carbonate (2 M, 0.8 mL). The reaction mixture was stirred at 80 °C under argon for 48 hours. A solution of saturated ammonium chloride (100 mL) was added and organic compounds were extracted with dichloromethane (2×100 mL). The combined organic phases were washed with a saturated solution of sodium chloride (250 mL), dried over anhydrous sodium sulfate, filtrated and concentrated under reduced pressure. The crude product was purified by a silicagel column chromatography (CH_2Cl_2/PE: 6.5/3.5) to give two orange solids **5** (Yield: 57% (0.20 g)) and **6** (Yield: 42% (0.13 g)). Characterizations of **5**: mp: 90 °C; IR (ν_{max}/cm^{-1}): 2923, 2853, 1591, 1548, 1492, 1461, 1329, 1282, 1180, 1070, 837; ^{1}H NMR (400 MHz, $CDCl_3$) δ (ppm): 8.12 (s, 2H), 7.38 (d, J=8.7 Hz, 4H), 7.31 (dd, J=8.2 and 7.8 Hz, 8H), 7.18 (d, J=7.8 Hz, 8H), 7.12 (d, J=8.7 Hz, 4H), 7.08 (t, J=7.3Hz, 4H), 2.75 (t, J=7.8 Hz, 4H), 1.65 (tt, J=7.3 and 6.9 Hz, 4H), 1.40-1.27 (m, 28H), 0.89 (t, J=6.8 Hz, 6H); ^{13}C NMR (100 MHz, $CDCl_3$) δ (ppm): 161.1, 148.1, 147.4, 145.9, 140.5, 133.3, 132.8, 129.9, 129.5, 127.2, 125.1, 123.6, 122.6, 32.0, 30.1, 29.7 (2C), 29.6 (2C), 29.5, 29.0, 22.8, 14.3; HRMS-MALDI (m/z): (M)$^{\bullet+}$ calcd for $C_{66}H_{72}N_6S_2$, 1012.5254, found 1012.5240; UV-vis (CH_2Cl_2) λ_{max}(ε) = 306 nm (49100 L.mol^{-1}.cm^{-1}) and 441 nm (49300 L.mol^{-1}.cm^{-1}); Characterizations of **6**: mp: <50 °C; IR (ν_{max}/cm^{-1}): 2962, 2924, 2853, 1592, 1550, 1492, 1465, 1330, 1261, 1095, 1071, 1018, 800; ^{1}H NMR (400 MHz, $CDCl_3$) δ (ppm): 8.12 (s, 1H), 8.08 (s, 1H), 7.37 (d, J=8.7 Hz, 2H), 7.30 (dd, J=8.2 and 7.3 Hz, 4H), 7.17 (dd, J=8.7 and 0.9 Hz, 4H), 7.12 (d, J=8.7 Hz, 2H), 7.08 (t, J=7.3 Hz, 2H), 2.74 (t, J=7.3 Hz, 2H), 2.69 (t, J=7.3 Hz, 2H), 1.75-1.65 (m, 4H), 1.39-1.19 (m, 28H), 0.88 (t, J=6.8 Hz, 3H), 0.87 (t, J=6.8 Hz, 3H); ^{13}C NMR (100 MHz, $CDCl_3$) δ (ppm): 161.5, 161.2, 148.2, 147.4, 146.1, 145.6, 140.6, 135.8, 133.5, 132.6, 132.8, 130.0, 129.6, 127.5, 127.1, 125.2, 123.7, 122.6, 32.1(2C), 30.9(2C), 30.5(2C), 29.8(2C), 29.7(2C), 29.5(2C), 29.4(2C), 29.0(2C), 22.8(2C), 14.3(2C); HRMS-MALDI (m/z): (M)$^{\bullet+}$ calcd for $C_{48}H_{58}BrN_5S_2$, 847.3317, found 847.3298 (100%); UV-vis (CH_2Cl_2) λ_{max}(ε) = 305 nm (34800 L.mol^{-1}.cm^{-1}), 354 nm (34000 L.mol^{-1}.cm^{-1}) and 441 nm (25100 L.mol^{-1}.cm^{-1})

Acknowledgements

C. Q, V. A.-R, C. D.-V, G. C and P. A thank the CNRS and the Ministry of French Research for funding the project. S.-H. C and J.W. P thanks the support of DARPA ZOE program (Grant No. W31P4Q-09-1-0012). Mr. J. Fromont and Dr. O. Galangau are thanked for technical assistance with calculations.

Notes and references

‡ The ND-2PA measured two-photon cross section (δ_{ND}) should be 2× larger than the z-scan measured degenerate two-photon cross section (δ_D). Detailed calculation is shown in reference [53] and [54]. However, due to the group velocity mismatch between the visible probe wavelengths and the near IR excitation wavelength, quantative determination of two-photon absorption cross sections using ND-2PA spectrometer is dubious.

§ Z-scan measurements showed negligible intensity-dependent nonlinear absorption behavior. This suggests the nonlinear response of these three chromophores at 830 nm is originated from two-photon absorption process and the contribution of excited state absorption or other higher nonlinear process is minimal.

1 R. A. Carboni and R. V. Lindsey, *J. Am. Chem. Soc.*, 1959, **81**, 4342.
2 G. L. Rusinov, R. I. Ishmetova, N. I. Latosh, I. N. Ganebnych, O. N. Chupakhin and V. A. Potemkin, *Russ. Chem. Bull.*, 2000, **49**, 355.
3 N. Saracoglu, *Tetrahedron*, 2007, **63**, 4199.
4 D. L. Boger, *Tetrahedron*, 1983, **39**, 2869.
5 D. L. Boger, *Chem. Rev.*, 1986, **86**, 781.
6 J. F. Vivat, H. Adams and J. P. A. Harrity, *Org. Lett.*, 2009, **12**, 160.
7 T. J. Sparey and T. Harrison, *Tetrahedron Lett.*, 1998, **39**, 5873.
8 E. Gomez-Bengoa, M. D. Helm, A. Plant and J. P. A. Harrity, *J. Am. Chem. Soc.*, 2007, **129**, 2691.
9 U. Rohr, J. Schatz and J. Sauer, *Eur. J. Org. Chem.*, 1998, **1998**, 2875.
10 L. A. Paquette, W. R. S. Barton and J. C. Gallucci, *Org. Lett.*, 2004, **6**, 1313.
11 Y. F. Suen, H. Hope, M. H. Nantz, M. J. Haddadin and M. J. Kurth, *J. Org. Chem.*, 2005, **70**, 8468.
12 R. Troschütz and J. Müller, *Synthesis*, 2006, **2006**, 1513.
13 L. I. Robins, R. D. Carpenter, J. C. Fettinger, M. J. Haddadin, D. S. Tinti and M. J. Kurth, *J. Org. Chem.*, 2006, **71**, 2480.
14 Y. H. Gong, F. Miomandre, R. Méallet-Renault, S. Badré, L. Galmiche, J. Tang, P. Audebert and G. Clavier, *Eur. J. Org. Chem.*, 2009, 6121.
15 G. Clavier and P. Audebert, *Chem. Rev.*, 2010, **110**, 3299.
16 A. Mangia, F. Bortesi and U. Amendola, *J. Heterocycl. Chem.*, 1977, **14**, 587.
17 S. C. Benson, L. Lee, L. Yang and J. K. Snyder, *Tetrahedron*, 2000, **56**, 1165.
18 C. Quinton, V. Alain-Rizzo, C. Dumas-Verdes, F. Miomandre and P. Audebert, *Electrochim. Acta*, 2013, **110**, 693.
19 C. Quinton, V. Alain-Rizzo, C. Dumas-Verdes, G. Clavier, F. Miomandre and P. Audebert, *Eur. J. Org. Chem.*, 2012, 1394.
20 W. Kaim, *Coord. Chem. Rev.*, 2002, **230**, 127.
21 U. Keppeler, S. Deger, A. Lange and M. Hanack, *Angew. Chem., Int. Ed. Engl.*, 1987, **26**, 344.
22 M. Glöckle and W. Kaim, *Angew. Chem. Int. Ed.*, 1999, **38**, 3072.
23 M. Glöckle, W. Kaim and J. Fiedler, *Z. Anorg. Allg. Chem.*, 2001, **627**, 1441.
24 O. Schneider and M. Hanack, *Angew. Chem.*, 1983, **95**, 804.
25 P. Audebert and F. Miomandre, *Chem. Sci.*, 2013, **4**, 575.
26 F. Miomandre, E. Lépicier, S. Munteanu, O. Galangau, J. F. Audibert, R. Méallet-Renault, P. Audebert and R. B. Pansu, *ACS Appl. Mater. Interfaces*, 2011, **3**, 690.
27 F. Miomandre, C. Allain, G. Clavier, J.-F. Audibert, R. B. Pansu, P. Audebert and F. Hartl, *Electrochem. Commun.*, 2011, **13**, 574.
28 C. Dumas-Verdes, F. Miomandre, E. Lépicier, O. Galangau, T. T. Vu, G. Clavier, R. Méallet-Renault and P. Audebert, *Eur. J. Org. Chem.*, 2010, **2010**, 2525.
29 F. Miomandre, R. Meallet-Renault, J. J. Vachon, R. B. Pansu and P. Audebert, *Chem. Commun.*, 2008, **16**, 1913.
30 Y. Kim, E. Kim, G. Clavier and P. Audebert, *Chem. Commun.*, 2006, 3612.
31 Y. Kim, J. Do, E. Kim, G. Clavier, L. Galmiche and P. Audebert, *J. Electroanal. Chem.*, 2009, **632**, 201.
32 S. Seo, Y. Kim, Q. Zhou, G. Clavier, P. Audebert and E. Kim, *Adv. Funct. Mater.*, 2012, **22**, 3556.
33 J. Malinge, C. Allain, L. Galmiche, F. Miomandre and P. Audebert, *Chem. Mater.*, 2011, **23**, 4599.

34 K. Hwang do, R. R. Dasari, M. Fenoll, V. Alain-Rizzo, A. Dindar, J. W. Shim, N. Deb, C. Fuentes-Hernandez, S. Barlow, D. G. Bucknall, P. Audebert, S. R. Marder and B. Kippelen, *Adv. Mater.*, 2012, **24**, 4445.
35 H. Alyar, M. Bahat, Z. Kantarcı and E. Kasap, *Comput. Theor. Chem.*, 2011, **977**, 22.
36 I. Janowska, F. Miomandre, G. Clavier, P. Audebert, J. Zakrzewski, K. H. Thi and I. Ledoux-Rak, *J. Phys. Chem. A*, 2006, **110**, 12971.
37 I. D. L. Albert, T. J. Marks and M. A. Ratner, *Chem. Mater.*, 1998, **10**, 753.
38 B. Jędrzejewska, P. Krawczyk, M. Pietrzak, M. Gordel, K. Matczyszyn, M. Samoć and P. Cysewski, *Dyes Pigm.*, 2013, **99**, 673.
39 K. D. Belfield, D. J. Hagan, E. W. Van Stryland, K. J. Schafer and R. A. Negres, *Org. Lett.*, 1999, **1**, 1575.
40 L. Antonov, K. Kamada, K. Ohta and F. S. Kamounah, *Phys. Chem. Chem. Phys.*, 2003, **5**, 1193.
41 Y. M. Poronik, G. Clermont, M. Blanchard-Desce and D. T. Gryko, *J. Org. Chem.*, 2013, **78**, 11721.
42 M. Albota, D. Beljonne, J. L. Brédas, J. E. Ehrlich, J. Y. Fu, A. A. Heikal, S. E. Hess, T. Kogej, M. D. Levin, S. R. Marder, D. McCord-Maughon, J. W. Perry, H. Röckel, M. Rumi, G. Subramaniam, W. W. Webb, X. L. Wu and C. Xu, *Science*, 1998, **281**.
43 L. Ventelon, M. Blanchard-Desce, L. Moreaux and J. Mertz, *Chem. Commun.*, 1999, 2055.
44 F. Hao, Z. Liu, M. Zhang, J. Liu, S. Zhang, J. Wu, H. Zhou and Y. Tian, *Spectrochim. Acta, Part A*, 2014, **118**, 538.
45 S. J. K. Pond, M. Rumi, M. D. Levin, T. C. Parker, D. Beljonne, M. W. Day, J.-L. Brédas, S. R. Marder and J. W. Perry, *J. Phys. Chem. A*, 2002, **106**, 11470.
46 M. Rumi, J. E. Ehrlich, A. A. Heikal, J. W. Perry, S. Barlow, Z. Hu, D. McCord-Maughon, T. C. Parker, H. Röckel, S. Thayumanavan, S. R. Marder, D. Beljonne and J.-L. Brédas, *J. Am. Chem. Soc.*, 2000, **122**, 9500.
47 F. Pop, J. Ding, L. M. L. Daku, A. Hauser and N. Avarvari, *RSC Adv.*, 2013, **3**, 3218.
48 J. Catalan, *J. Phys. Chem. B*, 2009, **113**, 5951.
49 M. Baruah, W. Qin, C. Flors, J. Hofkens, R. A. L. Vallée, D. Beljonne, M. Van der Auweraer, W. M. De Borggraeve and N. Boens, *J. Phys. Chem. A*, 2006, **110**, 5998.
50 W. Qin, M. Baruah, M. Sliwa, M. Van der Auweraer, W. M. De Borggraeve, D. Beljonne, B. Van Averbeke and N. Boens, *J. Phys. Chem. A*, 2008, **112**, 6104.
51 S. F. Mason, *J. Chem. Soc.*, 1959, 1263.
52 J. Waluk, J. Spanget-Larsen and E. W. Thulstrup, *Chem. Phys.*, 1995, **200**, 201.
53 R. A. Negres, J. M. Hales, A. Kobyakov, D. J. Hagan and E. W. Van Stryland, *Opt Lett*
54 *Opt Lett*, 2002, **27**.
55 J. M. Hales, D. J. Hagan, E. W. Van Stryland, K. J. Schafer, A. R. Morales, K. D. Belfield, P. Pacher, O. Kwon, E. Zojer and J. L. Bredas, *J Chem Phys*
56 *J Chem Phys*, 2004, **121**.
57 M. Parent, O. Mongin, K. Kamada, C. Katan and M. Blanchard-Desce, *Chem. Commun.*, 2005, 2029.
58 M. G. Vivas, D. L. Silva, L. De Boni, Y. Bretonniere, C. Andraud, F. Laibe-Darbour, J. C. Mulatier, R. Zalesny, W. Bartkowiak, S. Canuto and C. R. Mendonca, *J. Phys. Chem. B*, 2012, **116**, 14677.
59 J. Massue, J. Olesiak-Banska, E. Jeanneau, C. Aronica, K. Matczyszyn, M. Samoc, C. Monnereau and C. Andraud, *Inorg. Chem.*, 2013, **52**, 10705.
60 K. J. Schafer, J. M. Hales, M. Balu, K. D. Belfield, E. W. Van Stryland and D. J. Hagan, *J. Photochem. Photobiol., A*, 2004, **162**, 497.
61 Q. Bellier, N. S. Makarov, P. A. Bouit, S. Rigaut, K. Kamada, P. Feneyrou, G. Berginc, O. Maury, J. W. Perry and C. Andraud, *Phys. Chem. Chem. Phys.*, 2012, **14**, 15299.
62 P.-A. Bouit, G. Wetzel, G. Berginc, B. Loiseaux, L. Toupet, P. Feneyrou, Y. Bretonnière, K. Kamada, O. Maury and C. Andraud, *Chem. Mater.*, 2007, **19**, 5325.
63 B. H. Cumpston, S. P. Ananthavel, S. Barlow, D. L. Dyer, J. E. Ehrlich, L. L. Erskine, A. A. Heikal, S. M. Kuebler, I. Y. S. Lee, D. McCord-Maughon, J. Qin, H. Rockel, M. Rumi, X.-L. Wu, S. R. Marder and J. W. Perry, *Nature*, 1999, **398**, 51.

View Article Online
DOI: 10.1039/C5TC00531K